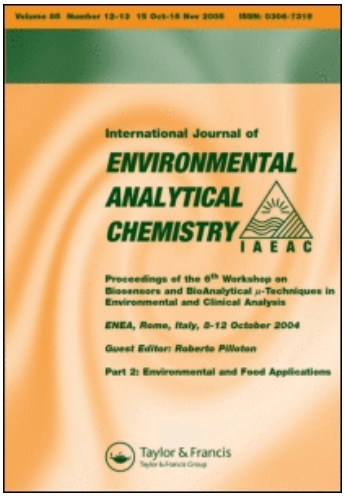

International Journal of Environmental Analytical Chemistry
Publication details, including instructions for authors and subscription information:
http://www.informaworld.com/smpp/title~content=t713640455

Amoxicillin removal from aqueous matrices by sorption with almond shell ashes

Vera Homem[a]; Arminda Alves[a]; Lúcia Santos[a]
[a] LEPÆ, Departamento de Engenharia Química, Faculdade de Engenharia da Universidade do Porto, Porto, Portugal

Online publication date: 22 October 2010

To cite this Article Homem, Vera , Alves, Arminda and Santos, Lúcia(2010) 'Amoxicillin removal from aqueous matrices by sorption with almond shell ashes', International Journal of Environmental Analytical Chemistry, 90: 14, 1063 — 1084
To link to this Article: DOI: 10.1080/03067310903410964
URL: http://dx.doi.org/10.1080/03067310903410964

Intern. J. Environ. Anal. Chem.
Vol. 90, Nos. 14–15, 10–20 December 2010, 1063–1084

Taylor & Francis
Taylor & Francis Group

Amoxicillin removal from aqueous matrices by sorption with almond shell ashes[1]

Vera Homem, Arminda Alves and Lúcia Santos*

LEPÆ, Departamento de Engenharia Química, Faculdade de Engenharia da Universidade do Porto, Rua Dr., Roberto Frias, 4200-465 Porto, Portugal

(*Received 30 November 2008; final version received 5 October 2009*)

The adsorption of the antibiotic amoxicillin at low concentration levels ($\mu g\,L^{-1}$ order) from aqueous solution on almond shell ashes has been investigated, either by kinetic or equilibrium assays. The effect of the adsorbent amount, initial concentration of the antibiotic, particle diameter (d_p) and temperature were considered to evaluate the adsorption capacity of the adsorbent. The results showed that amoxicillin sorption is dependent on these four factors. The adsorption process was relatively fast and equilibrium was established in about 12 hours. The optimum parameters for an initial concentration of $450\,\mu g\,L^{-1}$ were 50 mg of adsorbent, 303 K and $d_p < 600\,\mu m$. A comparison of kinetic models showed that pseudo-second order kinetics provides the best correlation of the experimental data. Isotherm data adjusted better to Langmuir equation, with an adsorption capacity of $2.5 \pm 0.1\,mg\,g^{-1}$ at 303 K. The desorption process was also evaluated (maximum efficiency of 5%). Thermodynamic parameters were calculated and the negative value of ΔH^0 and ΔG^0 showed that adsorption was exothermic and a spontaneous process.

Keywords: antibiotics; amoxicillin; adsorption; almond shell ashes

1. Introduction

Nowadays, one of the most important topics in the environmental field is water quality, because it is an essential resource for life. The amount of freshwater on Earth is limited, and its quality is under constant pressure. This fact has resulted in the demand for the quality protection of water resources, in an effort to prevent its contamination with pathogen agents and toxic compounds [1]. The attention has been diverted to the potential presence of pharmaceutical compounds in the environment. Residues of human and veterinary pharmaceuticals are presented in a variety of matrices, like surface, groundwater, soils and sediments [1,2]. The introduction of these compounds into the ecosystem, as parent compounds, metabolites or both forms conjugated, is related with the metabolic excretion, waste effluents of manufacturing processes and discharges from wastewater treatment plants (WWTPs), which are not often designed to remove these chemicals [2,3]. Recent studies revealed the presence of pharmaceuticals in the aquatic environment at

*Corresponding author. Email: lsantos@fe.up.pt

[1]This study was presented at the 5th European Conference on Pesticides and Related Organic Micropollutants in the Environment and the 11th Symposium on Chemistry and Fate of Modern Pesticides, Marseille, 22–25 October 2008.

ISSN 0306–7319 print/ISSN 1029–0397 online

DOI: 10.1080/03067310903410964
http://www.informaworld.com

levels of ng to $\mu g\,L^{-1}$ [3]. Although present at trace levels, these substances are sufficient to induce toxic effects in terrestrial and aquatic organisms.

Among a wide diversity of pharmaceutical compounds, antibiotics are a class of organic pollutants of extreme importance due to their intrinsic properties, which allow their persistence and bioaccumulation. On the other hand, they are suspected to be responsible for the appearance of resistance in natural bacterial populations [3,4]. Until now, the antibiotics concentration limits in the environment have not been regulated.

A high percentage of antibiotics is excreted unchanged. This is the case of the beta-lactam antibiotic, amoxicillin, which 80–90% is excreted unmodified [5]. From the class of penicillins, amoxicillin represents one of the most prescribed antibiotics in Europe and in the United States [6,7]. The extensive use of this antibiotic associated with difficulty in being metabolised enhances the environmental contamination. Amoxicillin has been detected in several matrices (WWTPs effluents [8,9], hospital effluents [8], river waters [8], sea waters [9]) and the toxic effects of this compound towards aquatic organisms have been recently reported [10]. Therefore, ecological risks of amoxicillin in the environment should not be underestimated. This is the main motivation to study amoxicillin in this work.

As mentioned above, most conventional WWTPs are not prepared for the treatment of wastewaters containing these kinds of substances [5]. Therefore, practical and economical solutions must be achieved in order to reduce the amount discharged daily into the ecosystems. A wide range of chemical and physical methods for organic compound removal from water matrices can be applied. Among these different processes are biodegradation, coagulation, sedimentation, filtration, oxidative processes or combinations of these procedures. However, some of these conventional techniques have limitations and are not effective or economically attractive. This is the case of biodegradation, because antibiotics and other pharmaceuticals are toxic to microorganisms [11]. An alternative is the application of adsorption processes. This technique has the advantage of removing the analytes instead of producing metabolites that are potentially more dangerous.

The adsorption efficiency is related to the adsorbent properties, namely surface area, porosity and pore diameter [12]. The most popular adsorbents are granular activated carbons (GACs), but their high cost and difficulty of regeneration are disadvantages [12–14]. Thus, the interest for alternative adsorbents grows with the purpose of finding low-cost adsorbents, as by-products or waste materials from industrial or agricultural processes. Hazelnuts, coconut, walnut, almond shells and others have been used for this purpose [14–16]. It is very important to take into account that some of these adsorbents require a previous activation treatment in order to increase their surface areas.

Few studies about antibiotic adsorption exist in the literature. Dutta *et al.* [17] studied the adsorption of β-lactam antibiotics using different types of polymeric resins and activated carbon, Ötker *et al.* [18] reported the use of a natural zeolite to adsorb one veterinary antibiotic (enrofloxacin) and Choi *et al.* [19] studied tetracycline removal with two different materials, coal-based carbon and coconut-based carbon. Putra *et al.* [20] reported the performance of activated carbon and bentonite for adsorption of amoxicillin from wastewater. They compared the adsorption efficiency of these two adsorbents and studied the kinetic and equilibrium of this process. They obtained 95% and 88% of removal, using activated carbon and bentonite, respectively. This study uses initial concentrations of $300\,mg\,L^{-1}$, which are far from the values found in domestic wastewaters or river waters. Therefore, the study could only be applied to pharmaceutical wastewaters. No data was found in literature about the use of almond shell, both in their natural state or with activation treatment, to remove antibiotics from

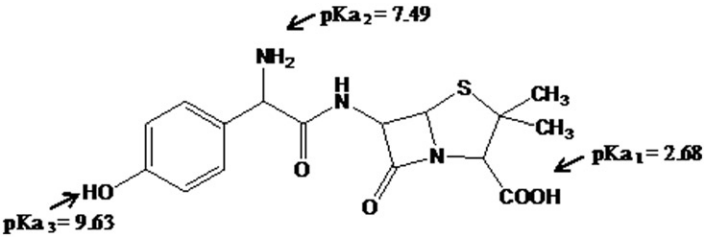

Figure 1. Amoxicillin structure and pKa values.

contaminated waters. Almond shells have been applied in the removal of heavy metals [15–16,21–22], dyes [23] and pentachlorophenol [24,25] from water matrices. In Portugal, annual almond production is close to 27,000 tonnes. Taking into account that each almond has about 50% of shell (in mass), a large amount of this agricultural by-product is available to be used as adsorbent material [25].

To our knowledge, no research has been yet conducted about the employment of almond shells as adsorbent for amoxicillin removal. The main objective of this work is to evaluate the capability of the almond shell ashes to remove amoxicillin [26] (Figure 1) from water matrices. In this study, batch experiments were performed in order to determine kinetics and equilibrium parameters, enabling the modelling of the process.

2. Experimental

2.1 *Chemicals and materials*

Amoxicillin, ≥900 μg per mg (ref. A8523), was obtained from Sigma-Aldrich (St. Louis, USA). Acetonitrile HPLC grade from Panreac (Barcelona, Spain) and *o*-phosphoric acid 85% p.a. from Pronalab (Lisbon, Portugal) were utilised.

Almond shells were a by-product from agricultural production obtained in the northern region of Portugal (Bragança).

2.2 *Standards preparation*

An aqueous stock solution of 56 mg L^{-1} of amoxicillin (AMOX) was prepared. From this, calibration standards with concentrations of 45, 112, 168, 224, 336, 392 and 448 μg L^{-1} were prepared in deionised water, previously filtered through 0.45 μm nylon filter membranes from Supelco (Sintra, Portugal). From the stock solution, a control standard of 448 μg L^{-1} was prepared weekly.

2.3 *Adsorbent preparation and characterisation*

The almond shells were first washed several times with deionised water to remove any surface impurities and then dried at 50°C for 72 hours. The shells were ground in a Retsch ZM 100 Mill and sieved in Endecotts Test Sieves (London, England). The size fraction between 1000 and 710 μm was burned in a furnace with an oxygen-poor atmosphere. The furnace temperature was increased at a certain rate from room temperature to 700°C and then, it was held for 2 hours. After this time, the furnace was cooled down to room temperature. The ashes obtained were sieved again, dried for 24 hours at 50°C and kept in dry conditions until the experiments.

Physical characterisation of the adsorbent was performed in order to understand the adsorption process. The distribution of the particle diameter was assessed by granulometry with a Coulter Counter-LS 230 Particle Size Analyser (Miami, USA). Apparent density, pore volume, surface area and average pore diameter were obtained by mercury porosimetry with a Quanta Chrome Pore Master (Boynton Beach, USA), while real density was determined by helium pycnometry. The adsorbent was also characterised by Fourier transform infrared spectroscopy (FTIR, Bomem MB Series, Arid-Zone™ – Quebec, Canada), X-ray photoelectron spectroscopy (XPS, VG Scientific ESCALAB 200A from CEMUP, Centro de Materiais da Universidade do Porto), scanning electron microscopy (SEM, FEI QUANTA 400 FEG ESEM also from CEMUP), thermogravimetry (Netzsch TG 209 F1 Iris® – Selb, Germany) and elemental analysis (CHNS Carlo Erba Instruments EA 1108 – Milan, Italy). The point of zero charged (pH_{PZC}) was determined through the pH drift method described by Rivera-Utrilla *et al.* [27].

2.4 *Analytical method*

Chromatographic analyses were performed using a Merck Hitachi LaChrom system (Darmstadt, Germany) equipped with an L-7100 pump, a manual Rheodyne 7725i loop injector and a diode array detector (DAD) L-7450. Data was acquired and processed by HSM D-7000, Version 3.1, software.

A reversed-phase (RP) C18 column, type Purospher® STAR (250 mm × 4 mm i.d., particle size: 5 μm), in combination with a guard column (4 mm × 4 mm i.d.) also Purospher® STAR were used. The mobile phase was composed of acetonitrile (5%) and *o*-phosphoric acid (pH = 2.5) in water (95%), running in isocratic conditions. The flow rate was 0.8 mL min^{-1} and the injection volume was 100 μL. The scanning wavelength range was 220–400 nm and the UV absorption of amoxicillin was measured at 230 nm. This method was based on a previous one, already described by Teixeira *et al.* [28].

2.5 *Adsorption and desorption procedure*

In the adsorption process, the effect of almond shell ashes amount (0.8–10 g L^{-1}), initial amoxicillin concentration (200–750 μg L^{-1}), temperature (283–303 K) and particle size of the adsorbent ($d_p < 600$ μm and 600 μm $< d_p <$ 770 μm) were investigated by batch experiments for a specific period of contact time (0–400 min).

For the kinetic studies, which allowed the determination of the equilibrium time, all experiments were carried out keeping constant the adsorbent mass (50 mg). The ashes, with a defined particle size, were equilibrated with 20 mL of water for 2 hours in closed erlenmeyer flasks. After this period, samples were spiked with the stock solution of amoxicillin to the required initial concentration. The flasks were placed inside a Lovibond thermostatic cabinet (Dortmund, Germany) at constant temperature and the solutions were stirred at 120 rpm with magnetic bars for a certain period of time. At various time intervals, the suspension was filtrated with VWR quantitative filter papers with particle retention between 5–10 μm (West Chester, USA) and subsequently, with a syringe filters 0.2 μm PTFE membrane (West Chester, USA).

After these assays, equilibrium time was set and the adsorption isotherms were determined, varying the amoxicillin/adsorbent mass ratio. The experimental procedure is similar to the one described above.

It is also important to notice that, in this work, three blanks were realised. It was checked if the filter paper contributed to the amoxicillin adsorption, if the water used for the solutions preparation did not contain the compound to analyse and whether the almond shell ashes in solution did not release compounds that could interfere in the identification and quantification of the antibiotic under study.

In order to study the desorption process, the shell ashes from the adsorption assays were removed and immersed in 20 mL of deionised water, previously filtrated, and maintained at constant temperature for 12 h. All experiments were performed in duplicate and the samples were kept at 4°C until quantification.

The concentration retained in the adsorbent (q_e in mg g^{-1}) was evaluated using:

$$q_e = \frac{(C_0 - C_e)V}{m} \tag{1}$$

where C_0 and C_e are the concentrations of amoxicillin at initial and equilibrium, respectively (mg L^{-1}), V the volume of the aqueous phase (L) and m is the mass of adsorbent used (g).

The data analysis was carried out using two functions, determination coefficient, R^2, and normalised standard deviation, SD, defined as:

$$\%\mathrm{SD} = \sqrt{\frac{\left(\frac{q_{\mathrm{exp}} - q_{\mathrm{calc}}}{q_{\mathrm{exp}}}\right)^2}{n-1}} \times 100 \tag{2}$$

where the subscripts exp and calc refer to the experimental and calculated values and n the number of data points.

3. Results and discussion

3.1 *Analytical method*

The retention of amoxicillin was 11.4 ± 0.4 min and the total run time of the HPLC-DAD method was 13 minutes. The analytical method was validated and uncertainties estimated according to the EURACHEM/CITAC guide [29] (Table 1).

The precision was evaluated either by intermediate precision or repeatability. Intermediate precision was determined using inter-day analysis (6 days) at three concentration levels, while repeatability was obtained from six replicate analyses at the same three levels in the shortest period of time. Accuracy was expressed through analytical

Table 1. Validation parameters for amoxicillin analysis by HPLC-DAD.

Linearity range (μg L^{-1})	45–450		
R^2	0.9941 ($N = 7$)		
Detection limit (μg L^{-1})[a]	29		
Precision (%CV)	112 μg L^{-1}	224 μg L^{-1}	448 μg L^{-1}
Intermediate precision	4.8	5.5	4.4
Repeatability	8.7	3.1	2.9
Accuracy (% Recovery)	101	89	92

[a]Calculated from the calibration curve.
N: number of calibration standards; R: coefficient of determination; CV: coefficient of variation.

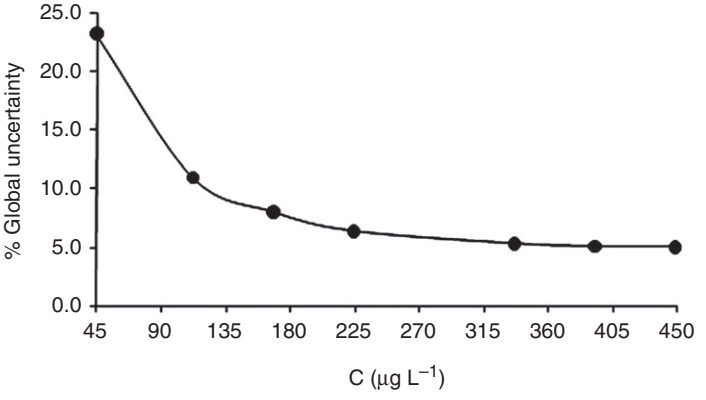

Figure 2. Global uncertainty estimated by the EURACHEM approach.

recovery tests (the observed value divided by the expected value), using standard addition method.

The global uncertainty is concentration dependent and is expressed in Figure 2.

3.2 *Almond shell ashes characterisation*

The first step of this work was a preliminary characterisation of the adsorbent material, so that the adsorption process could be interpreted and allow the performance comparison between other sorbents. Table 2 shows the main characteristics of the almond shell ashes used.

According to the IUPAC recommendation [30], the pores can be classified in macropores (>50 nm), mesopores (>2 nm and <50 nm) and micropores (<2 nm). The pore diameter range of the adsorbent used allows its classification in macro and mesopores. Estevinho *et al.* [25] and Bulut *et al.* [22] characterised almond shell, which had not suffered any kind of activation treatment. A total surface area of 10.95 and 4.11 $m^2 g^{-1}$ were achieved, respectively. There is a significant increase in surface area from the shells to the almond ashes. Natural polymeric resins [17] have areas between 330–800 $m^2 g^{-1}$, granular activated carbons about 1200 $m^2 g^{-1}$ and alumina 200–300 $m^2 g^{-1}$ [31]. These kinds of adsorbents usually have a total surface area much larger, but as mentioned above, they are extremely expensive and it is difficult to do their regeneration. The scanning electron microscope images show the morphology of almond shell ashes (Figure 3). As can be seen, the adsorbent particles have uniform shapes and dimensions. It is also possible to identify pores (mainly macro and mesopores) throughout the surface, creating advantageous conditions for adsorption (it may occur not only at the sorbent surface, but also on the intraparticle network).

The point of zero charge was also determined and it can be used to explain the interaction between adsorbent and adsorbate. The pH_{PZC} was determined as 7.02 ± 0.06. The pH solution was 6.5, so in the adsorption experiments, the adsorbent surface is positively charged. According to the theoretical pKa values (Figure 1), at this pH, amoxicillin is predominantly in a negative form ($-COO^-$), although a percentage of the amino group has been already deprotonated (NH_2 form). Hence, positive surface of the adsorbent attracts the negatively charged group of amoxicillin.

Table 2. Main characteristics of the almond shell ashes used in this work.

Properties	
Real density	$1.77\,g\,cm^{-3}$
Apparent density	$0.95\,g\,cm^{-3}$
Total surface area	$78.50\,m^2\,g^{-1}$
Total interparticle porosity	0.63%
Total intraparticle porosity	32.27%
Total porosity	32.90%
Pore diameter range	10238–4 nm
Pore diameter (mean)	18 nm
pH_{PZC}	7.02 ± 0.06
Elemental analysis[a] (wt%)	
C	90.94 ± 0.03
H	8.07 ± 0.10
N	0.34 ± 0.07
O[b]	1.10 ± 0.02
Atomic percentage[c] (mol%)	
C	85.47
N	0.26
O	14.28
Thermogravimetry analysis[d] (wt%)	
Volatile matter	81.90
Fixed carbon	18.10
Ashes	≈0

[a]Dry and ash free basis.
[b]By difference.
[c]As determined by XPS; C+N+O = 100%.
[d]Dry basis.

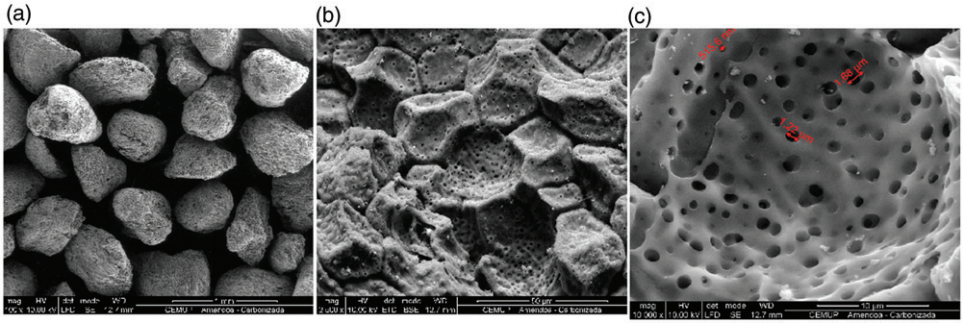

Figure 3. SEM images of almond shells ashes (a) amplified 100 times, (b) amplified 2500 times, (c) amplified 10,000 times.

Chemical characterisation of the sorbent surface was performed by FTIR and XPS analysis. The FTIR spectrum (*not shown*) had poor resolution and practically did not show any remarkable IR band. However, low resolution bands appear in the characteristic region of C–O bond (stretching) ~1000–1250 cm^{-1}, C-H (bending) ~1350–1450 cm^{-1} and

Table 3. Relative intensities of XPS C1s, O1s and N1s peaks.

	Binding energy (eV)					
	This work	In reference	Ref.	Surface group	Description	% Bond
C 1*s*	284.4	284.6	[32–34]	C–C, C–H	Graphitic carbon	58.5
	286.1	286.0–286.3	[32–34]	C–OH, C–O	Phenol, alcohol and ether	15.1
	287.4	286.3–287.6	[32–34]	C=O, C–N	Carbonyl, quinone, carbon-nitrogen structures	13.0
	288.8	288.8–289.1	[32–34]	COO	Carboxyl and ester	7.5
	290.3	290.5–291.2	[32–34]	C=O, C=C	Carbonate, CO or CO_2 occluded, π-electrons in the aromatic ring	3.4
	291.5	291.0–291.6	[32,35]	π–π transitions	Transition due to conjugation	2.5
O 1*s*	531.9	531.0–531.9	[32,34,36]	C=O	Carbonyl and quinone	44.6
	532.3	532.3–532.8	[34]	COOR	Esters and anhydrides	7.5
	533.8	533.2–533.8	[36]	C–O–R	Oxygen singly bounded to carbon in aromatic rings, phenol, alcohol and ether	19.3
	535.2	534.3–535.4	[32,34]	COO	Carboxyl	22.4
	537.0	537.0	[36]	C=O	CO or CO_2 occluded	6.3
N 1*s*	399.9	400.1	[32]	C–N	Carbon-nitrogen structures	100

the presence of dissolved CO_2 ~2250 cm^{-1}. For higher frequency values, a wide band occurs, which does not identify any specific bond.

The binding energies of C1s, O1s and N1s levels of the adsorbent material were determined by XPS. The peaks obtained were deconvoluted and a detailed chemical-bond analysis was realised by curve fitting with a least squares method using the XPSPEAK Version 4.1. The results are expressed in Table 3.

The XPS analysis proved the existence of functional groups in the adsorbent material (e.g. C–OH, COOH) that can establish hydrogen bonds with some amoxicillin groups (phenol, primary and secondary amine). Moreover, the XPS showed the existence of π-electrons on the adsorbent surface that can also interact with the amoxicillin aromatic ring. Another possibility, although less probable, is the reaction between a carbonyl group of the adsorbent (from aldehydes or ketones) and the primary amine of amoxicillin, to form an imine.

3.3 *Effect of adsorbent amount*

This parameter is related to the adsorption capacity of the adsorbent under study, for a determined analyte concentration. The adsorbent mass optimisation was performed, changing the amount of almond shell ashes between 0.8 and 10 g L^{-1} and keeping all other factors constant. Figure 4 shows the results of this analysis.

The increasing in the adsorbent amount results in greater removal efficiency and in a decrease of the adsorbed amount. It is important to note that the number of available sites for adsorption increases by increasing the adsorbent amount, and consequently, the

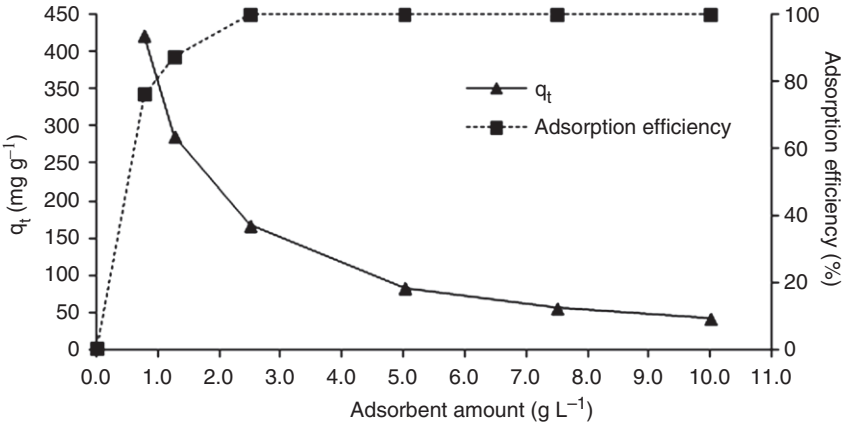

Figure 4. Adsorbent mass optimisation for a contact time of 400 min, amoxicillin concentration of 450 μg L^{-1}, $d_p < 600$ μm, 303 K and 120 rpm.

efficiency removal is also increased. On the other hand, the reduction in the amount adsorbed is related to the adsorption unsaturation throughout the adsorption process.

A mass of 50 mg, which corresponds to 2.5 g L^{-1}, was fixed in order to minimise the amount of sorbent material, but maintaining high removal efficiency. For the rest of the study, this amount was considered as optimum value for amoxicillin removal.

Intending to evaluate the effect of the pre-treatment, a preliminary study was performed with almond shell, using 100 mg of this adsorbent in the same experimental conditions (contact time of 400 min, amoxicillin concentration of 450 μg L^{-1}, dp < 600 μm, 303 K and 120 rpm). The adsorption efficiency achieved with pre-treatment (97%) is much higher than that obtained using natural almond shell (8%), explaining the interest of the pre-treatment applied in this study.

3.4 *Contact time and amoxicillin concentration*

The evaluation of the contact time required to reach the equilibrium was also studied. The amount adsorbed was determined as a function of contact time and initial concentration of amoxicillin (expressed as AMOX/adsorbent mass ratio). Figure 5 shows the results. At the beginning, the adsorption process was very fast, decreasing gradually until the equilibrium has been reached. As expected, to higher initial concentrations and consequently, higher AMOX/adsorbent mass ratio, the time needed to achieve the equilibrium was greater. After 400 min, an average removal efficiency of 97% was already obtained. However, to ensure the equilibrium between the two phases (solid-liquid) a contact time of 720 min (12 hours) was considered.

Changing the ratio mass AMOX/adsorbent between 0.08 and 0.30 mg g^{-1}, the amount adsorbed increases from 0.081 to 0.278 mg g^{-1}. This may be attributed to an increase in the mass transfer driving force, in order to overcome mass transfer resistances of amoxicillin between the bulk solution and the particle surface. Furthermore, it is known that for high concentrations (keeping constant the adsorbent mass), there are fewer active sites available

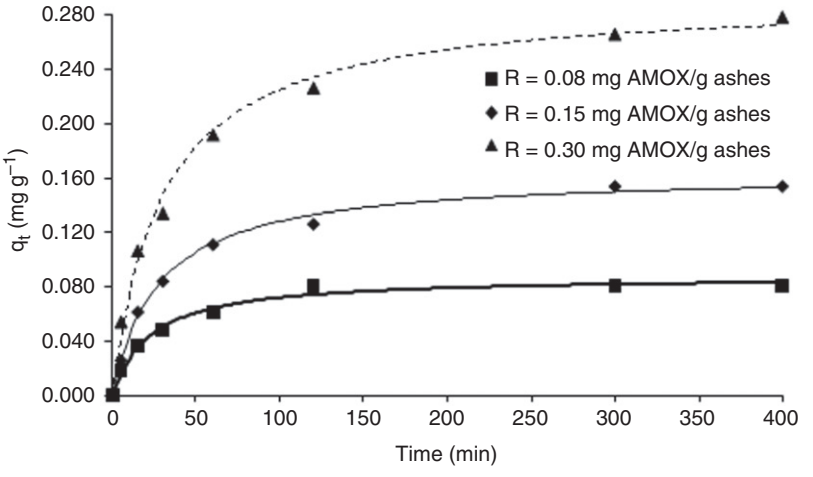

Figure 5. Effect of the contact time on the adsorption process at different AMOX/adsorbent mass ratio at 303 K (adsorbent mass = 50 mg, $d_p < 600\,\mu m$, 120 rpm).

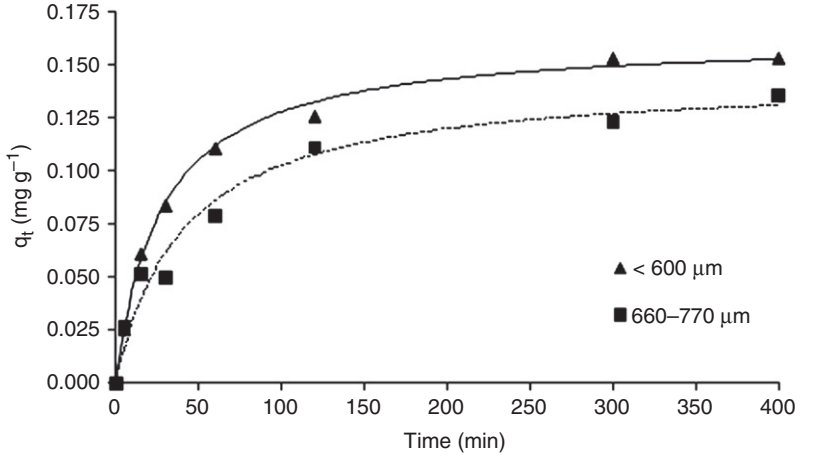

Figure 6. Effect of particle size on amoxicillin adsorption (450 $\mu g\,L^{-1}$ amoxicillin concentration, 50 mg of adsorbent, 303 K and 120 rpm).

to adsorption and removal efficiency is decreased. Once again, this fact proves that adsorption is affected by the initial analyte concentration.

3.5 *Effect of adsorbent particle size*

Experiments were also carried out to evaluate the effect of almond shell ashes particle size in the adsorption process. Two different particle sizes were tested: diameters less than 600 μm and 600–770 μm. Figure 6 shows the experimental results obtained.

The amount adsorbed increased from 0.136 to 0.153 $mg\,g^{-1}$ with the decrease in the particle size. Similarly, greater removal efficiency was achieved with smaller particle sizes (89 to 100%). It is important to take into account that smaller particles have large surface

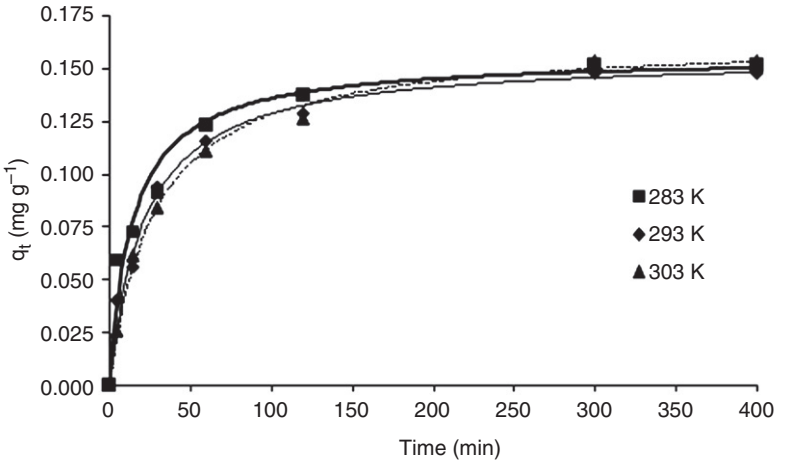

Figure 7. Effect of temperature on amoxicillin adsorption (450 μg L^{-1} amoxicillin concentration, 50 mg of adsorbent, $d_p < 600$ μm and 120 rpm).

areas. This fact suggests that the antibiotic studied should be adsorbed in the surface active sites of the adsorbent particles.

3.6 *Effect of temperature*

The effect of temperature on the adsorption was studied by a series of experiments conducted at 283, 293 and 303 K, using 450 μg L^{-1} initial amoxicillin concentration and $d_p < 600$ μm. Considering the results from Figure 7, the temperature does not seem to influence the adsorption process. However, further analyses of the thermodynamic results (Topic 3.9) suggest that the adsorption process may be exothermic. Hence, when the temperature increases, it is expected that the maximum adsorption capacity decreases and this behaviour was found when q_{max} (from isothermic models) was calculated.

3.7 *Adsorption kinetic modelling*

The study of adsorption kinetics intends to be a useful tool in the description of the solute uptake rate and, consequently in the residence time of the adsorbate at the solid-liquid interface. The kinetics of amoxicillin adsorption on the almond shell ashes was analysed using five different models: pseudo-first order, pseudo-second order, Elovich, external diffusion and intraparticle diffusion. The adsorption mechanism and the potential rate controlling steps were also investigated in this study.

3.7.1 *Adsorption reaction models*

These models were derived assuming that chemical reaction is the rate controlling step.

The pseudo-first order equation. The pseudo-first order chemical adsorption process is expressed as follows [37]:

$$\frac{dq_t}{dt} = k_1(q_e - q_t) \tag{3}$$

After integration, applying boundary conditions $q_t = 0$ at $t = 0$ and $q_t = q_t$ at $t = t$, this equation becomes

$$q_t = q_e(1 - e^{-k_1 t}) \tag{4}$$

where q_t and q_e are the adsorption capacities at time t and at equilibrium, respectively ($mg\,g^{-1}$) and k_1 is the rate constant of pseudo-first order adsorption ($L\,min^{-1}$). In this study, the values ranged between 0.080–0.261 $mg\,g^{-1}$ from q_e and 0.019–0.043 min^{-1} for k_1.

The pseudo-second order equation. The pseudo-second order kinetic rate equation is expressed as [37]:

$$\frac{dq_t}{dt} = k_2(q_e - q_t)^2. \tag{5}$$

Integrating between $q_t = 0$ at $t = 0$ and $q_t = q_t$ at $t = t$, the equation becomes

$$q_t = \frac{q_e^2 k_2 t}{1 + q_e k_2 t} \tag{6}$$

where q_t and q_e are the adsorption capacities at time t and at equilibrium ($mg\,g^{-1}$) and k_2 is the rate constant ($g\,mg^{-1}\,min^{-1}$). In this case, the rate constant calculated ranged from 0.11 and 0.53 $g\,mg^{-1}\,min^{-1}$, while the adsorption capacity from 0.087 and 0.292 $mg\,g^{-1}$.

The Elovich equation. The Elovich model is generally expressed as [38]:

$$\frac{dq_t}{dt} = \alpha e^{-\beta q_t}. \tag{7}$$

Applying the same boundary conditions mentioned in the prior model, the integrated equation will be expressed as follows:

$$q_t = \frac{1}{\beta}\ln(1 + \alpha\beta t) \tag{8}$$

where q_t is the adsorption capacity at time t ($mg\,g^{-1}$), α is the initial adsorption rate ($mg\,g^{-1}\,min^{-1}$) and β is the desorption constant ($g\,mg^{-1}$). Applying this model to the amoxicillin adsorption results, it was verified that the initial adsorption rate lies between 0.007 and 0.044 $mg\,g^{-1}\,min^{-1}$ and the desorption constant between 18 and 65 $g\,mg^{-1}$.

Table 4 provides a comparison between the adsorption kinetic parameters for these three different models. The models were fitted to the experimental data, using a non-linear analysis (Solver Excel, Microsoft Office Excel 2007).

The pseudo-first order model did not fit properly the whole range of contact times under investigation, but only the first experimental points (over the initial 30 minutes). This fact was also mentioned in other adsorption studies [22,39]. The Elovich model does not predict any mechanism, but had been used to describe chemical adsorption on heterogeneous adsorbents. This model predicts more correctly the behaviour across the studied range. As mentioned above, the β constant is related with desorption. As the initial amoxicillin concentration increases, the β constant decreases, reflecting a decrease in the amount of antibiotic to be desorbed per unit of adsorbent mass.

The model that best predicts the adsorption behaviour is the pseudo-second order. The validity of this affirmation is supported by the high values of determination coefficients and the lowest values of the normalised standard deviations. The values of the

Table 4. Pseudo first-order, pseudo second-order and Elovich kinetic parameters for amoxicillin adsorption at different initial concentrations, temperatures and particle diameter.

		Pseudo-first order				Pseudo-second order				Elovich Model				
Parameters	q_e, exp ($mg\,g^{-1}$)	q_e, calc ($mg\,g^{-1}$)	k_1 (min^{-1})	R^2	SD%	q_e, calc ($mg\,g^{-1}$)	k_2 ($g\,(mg\,min)^{-1}$)	R^2	SD%	q_e, calc ($mg\,g^{-1}$)	α ($mg\,(g\,min)^{-1}$)	β ($g\,mg^{-1}$)	R^2	SD%
C_0 ($\mu g\,L^{-1}$)[a]														
200	0.081	0.080 ± 0.003	0.033 ± 0.004	0.982	15.3	0.087 ± 0.003	0.53 ± 0.08	0.989	6.3	0.087	0.011 ± 0.005	65 ± 8	0.967	11.6
450	0.153	0.146 ± 0.006	0.028 ± 0.004	0.980	13.0	0.163 ± 0.003	0.22 ± 0.02	0.998	3.1	0.161	0.013 ± 0.003	32 ± 2	0.989	14.3
750	0.278	0.261 ± 0.012	0.025 ± 0.004	0.976	19.0	0.292 ± 0.008	0.11 ± 0.01	0.994	10.3	0.285	0.021 ± 0.003	18 ± 1	0.995	5.4
T (K)[b]														
283	0.152	0.143 ± 0.008	0.043 ± 0.010	0.942	21.2	0.155 ± 0.007	0.43 ± 0.11	0.971	14.2	0.158	0.044 ± 0.015	42 ± 4	0.985	6.6
293	0.148	0.141 ± 0.006	0.035 ± 0.005	0.976	17.1	0.155 ± 0.005	0.31 ± 0.05	0.990	11.5	0.156	0.020 ± 0.006	37 ± 4	0.978	11.2
303	0.153	0.146 ± 0.006	0.028 ± 0.004	0.980	13.0	0.163 ± 0.003	0.22 ± 0.02	0.998	3.1	0.161	0.013 ± 0.003	32 ± 2	0.989	14.3
d_p (μm)[c]														
< 600	0.153	0.146 ± 0.006	0.028 ± 0.004	0.980	13.0	0.163 ± 0.003	0.22 ± 0.02	0.998	3.1	0.161	0.013 ± 0.003	32 ± 2	0.989	14.3
600–770	0.136	0.128 ± 0.008	0.019 ± 0.004	0.962	26.6	0.144 ± 0.009	0.17 ± 0.05	0.972	20.4	0.136	0.007 ± 0.002	34 ± 4	0.980	12.0

[a]Experiments at 303 K, $d_p < 600\,\mu m$ and 120 rpm.
[b]Experiments at $450\,\mu g\,L^{-1}$ initial concentration of amoxicillin, $d_p < 600\,\mu m$ and 120 rpm.
[c]Experiments at 303 K, $450\,\mu g\,L^{-1}$ initial concentration of amoxicillin and 120 rpm.

second order rate constants were found to decrease from 0.53 to 0.11 $g\,mg^{-1}\,min^{-1}$ as the initial concentration increased from 200 to 750 $\mu g\,L^{-1}$. For the lowest initial concentrations, the collisions between molecules are less probable, allowing them to attach to the active sites, in a short period of time. These results show the consistence with the previous ones, showing the process dependence of initial concentration.

Because pseudo-second order kinetics predicts the adsorption behaviour and the rate constant (k_2) is independent of particle diameter, but strongly dependent on the sorbate concentration in solution and temperature, this study suggests that chemisorption is the rate-controlling step [40]. Chemisorption involves electron transfer, equivalent to the formation of a chemical bond between adsorbate and adsorbent surface.

As mentioned previously, Putra *et al*. [20] studied the performance of activated carbon and bentonite for adsorption of amoxicillin. Their study showed that the kinetic model of pseudo-second order fits the experimental data quite well, which corroborates the results obtained.

3.7.2 *Adsorption diffusion models*

Adsorption, whether physical or chemical, involves diffusion processes. The adsorbate must be diffused from the bulk solution to the boundary layer surrounding the adsorbent and then into the adsorption sites. Therefore, the diffusion process can be controlled by one or more of the following steps: bulk diffusion transport, external diffusion and/or intraparticle diffusion [13].

In the bulk diffusion, the adsorbate is transported through the bulk solution to the film surrounding the adsorbent. This resistance is usually reduced by stirring the solution, because the concentration gradient is reduced too. After this, the adsorbate should pass through the boundary layer surrounding the adsorbent to its surface – external diffusion. The diffusion rate is directly related to the thickness of the boundary layer (in thinner layers the diffusion rate is higher). In the intraparticle diffusion the adsorbate should be carried through the pores to the adsorption sites. The intraparticle transportation may occur by pore diffusion or by surface diffusion. After all these steps, the adsorbate will be attached to the adsorbent surface at available sites – adsorption.

As mentioned above, bulk diffusion and adsorption are rarely rate-limiting steps [13]. So, external and intraparticle diffusion are the concern mechanisms in this study.

The intraparticle diffusion model. Weber and Morris proposed a model to determine the rate constant for intraparticle diffusion [22,37]:

$$q_t = k_{id} t^{1/2} + C \tag{9}$$

where k_{id} is the initial rate of adsorption controlled by intraparticle diffusivity ($mg\,g^{-1}\,min^{-1/2}$) and C is the estimate of the boundary layer thickness. In this study, the values of the initial rate of adsorption lied between 0.004 and 0.013 $mg\,g^{-1}\,min^{-1/2}$.

The external (*film*) *diffusion model*. Doing a balance mass over the batch reactor, considering spherical-particle geometry, it was obtained this rate equation for film diffusion as limiting step:

$$\frac{dC_t}{dt} = -k_{fd}\frac{3m}{V\rho r}(C_t - C_s) \tag{10}$$

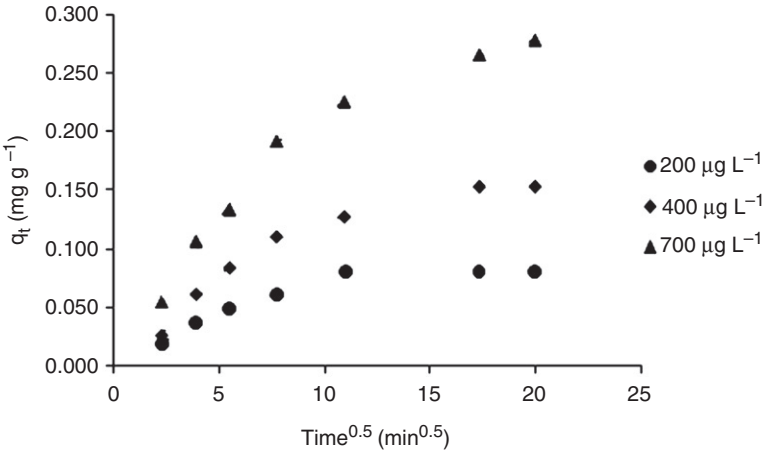

Figure 8. Intraparticle diffusion model (50 mg of adsorbent, 303 K, $d_p < 600$ µm and 120 rpm).

where C_t and C_s are the concentrations of the adsorbate in the bulk and at the particle surface, respectively (mg L^{-1}), k_{fd} is the coefficient of mass transfer in the film (cm min^{-1}), m is the mass of adsorbent (g), V the volume of the aqueous phase (cm^3), ρ is the apparent density of the adsorbent particle (g cm^{-3}) and r the average radius of the particle (cm).

Assuming that adsorbate concentration at particle surface is negligible at small values of time compared with the concentration of the bulk, the previous equation can be integrated between $C_t = C_0$ at $t = 0$ and $C_t = C_t$ at $t = t$:

$$C_t = C_0 e^{-k_{fd}\frac{3m}{V\rho r}t}. \tag{11}$$

As mentioned above, diffusion from the bulk liquid phase to the adsorbent surface and from this solid-liquid interface to the interior of the solid particles can play an important role in the adsorption mechanism.

According to the intraparticle model applied in this study, the diffusion occurs in the porous structure of the adsorbent and it is described by Fick's second law [38]. The plot of amoxicillin adsorbed, q_t, versus $t^{0.5}$ is presented for different initial concentrations at Figure 8. It was expected that this model was linear. However, it shows that this is not true, suggesting that intraparticle diffusion was not rate-controlling step.

The other model studied was external diffusion. If the adsorption process was controlled by external resistance, the plot of C_t/C_0 versus time should be linear, which was not confirmed. This model only fits adequately the first experimental points, indicating that external diffusion was not the rate-controlling step in the whole range studied, but probably in the first minutes. Table 5 presented the values of rate constants for those models presented above.

3.8 *Adsorption isotherms*

The solute distribution in the equilibrium is represented by a relationship between the amount of solute in the solid phase (q_e) and the final solute concentration in the liquid

Table 5. Intraparticle diffusion and external diffusion kinetic parameters for amoxicillin adsorption at different initial concentrations, temperatures and particle diameter.

		Intraparticle diffusion					External diffusion			
Parameters	q_e, exp ($mg\,g^{-1}$)	q_e, calc ($mg\,g^{-1}$)	k_{id} ($mg\,g^{-1}\,min^{-1/2}$)	C ($mg\,g^{-1}$)	R^2	SD%	q_e, calc ($mg\,g^{-1}$)	k_{fd} ($cm\,min^{-1}$)	R^2	SD%
C_0 ($\mu g\,L^{-1}$)[a]										
200	0.081	0.095	0.004 ± 0.001	0.018 ± 0.008	0.982	15.3	0.081	0.128 ± 0.012	0.983	15.7
450	0.153	0.175	0.007 ± 0.001	0.026 ± 0.012	0.980	13.0	0.153	0.098 ± 0.010	0.981	15.9
750	0.278	0.311	0.013 ± 0.002	0.044 ± 0.020	0.976	19.0	0.299	0.072 ± 0.011	0.977	25.3
T (K)[b]										
283	0.152	0.175	0.007 ± 0.001	0.042 ± 0.014	0.942	21.2	0.152	0.149 ± 0.026	0.948	20.7
293	0.148	0.171	0.007 ± 0.001	0.033 ± 0.014	0.976	17.1	0.148	0.126 ± 0.015	0.978	18.6
303	0.153	0.175	0.007 ± 0.001	0.026 ± 0.012	0.980	13.0	0.153	0.098 ± 0.010	0.981	15.9
d_p (μm)[c]										
< 600	0.153	0.175	0.007 ± 0.001	0.026 ± 0.012	0.980	13.0	0.153	0.098 ± 0.010	0.981	15.9
600–770	0.136	0.148	0.007 ± 0.001	0.017 ± 0.008	0.962	26.6	0.152	0.050 ± 0.009	0.963	25.8

[a]Experiments at 303 K, $d_p < 600\,\mu m$ and 120 rpm.
[b]Experiments at $450\,\mu g\,L^{-1}$ initial concentration of amoxicillin, $d_p < 600\,\mu m$ and 120 rpm.
[c]Experiments at 303 K, $450\,\mu g\,L^{-1}$ initial concentration of amoxicillin and 120 rpm.

phase (C_e), at constant temperature. This relationship is called isotherm. Four adsorption isotherms were investigated in this study: Linear, Langmuir, Freundlich and Temkin.

3.8.1 *Linear isotherm*

The simplest model describes the solute accumulation in the adsorbent as being directly proportional to the equilibrium concentration in the solution.

$$q_e = K_d C_e \tag{12}$$

where q_e is amount of solute adsorbed ($mg\,g^{-1}$), C_e the equilibrium concentration ($mg\,L^{-1}$) and K_d is the distribution coefficient ($L\,g^{-1}$). This model is usually applied to the adsorption of solutes in very low concentrations.

In this case, this model does not fit the experimental data ($R^2 < 0.850$).

3.8.2 *Langmuir isotherm*

Langmuir developed a model that presumes the formation of a monolayer on the adsorbent surface. In this model, it is assumed that the adsorption energy of each molecule is equal and independent of the coverage degree of the surface, the adsorption occurs in specific sites of the adsorbent and once occupied, no more adsorption takes place at that site [37]. This model may be represented as:

$$q_e = \frac{q_{\max} K_L C_e}{1 + K_L C_e} \tag{13}$$

where $q_{\max}$ is the monolayer capacity ($mg\,g^{-1}$) and K_L is the adsorption equilibrium constant ($L\,mg^{-1}$). Applying this model to the amoxicillin adsorption results, it was verified that $q_{\max}$ lies between 2.5 and $3.6\,mg\,g^{-1}$ and K_L between 1.7 and $2.0\,L\,mg^{-1}$.

3.8.3 *Freundlich isotherm*

Freundlich presented a model to describe the equilibrium relationship between the amount of solute in the solid and liquid phase. Although the model is empirical, it is quite precise to describe systems where adsorption in heterogeneous surfaces occurs [37]. The isotherm is expressed by the following equation:

$$q_e = K_f C_e^{1/n} \tag{14}$$

where K_f is the adsorption equilibrium constant ($mg\,g^{-1}\,(mg\,L^{-1})^{-1/n}$) and n the Freundlich constant. In this study, these parameters ranged between 1.24 and $2.23\,mg\,g^{-1}$ for K_f and 2.3 and 2.6 for n.

3.8.4 *Temkin isotherm*

This model takes into account the adsorbate-adsorbent interactions, and consequently, the variation of the heat adsorption with the adsorption surface coverage degree [37]. Temkin isotherm is represented as:

$$q_e = \frac{RT}{b} \ln(AC_e) \tag{15}$$

Table 6. Linear, Langmuir, Freundlich and Temkin isotherm parameters (450 μg L^{-1} initial concentration of amoxicillin, $d_p < 600$ μm and 120 rpm).

	Linear isotherm			Langmuir isotherm				Freundlich isotherm				Temkin isotherm			
T (K)	K_d ($L\,g^{-1}$)	R^2	SD%	q_{max} ($mg\,g^{-1}$)	K_L ($L\,mg^{-1}$)	R^2	SD%	K_f ($mg\,g^{-1}$)	n	R^2	SD%	A ($L\,mg^{-1}$)	B ($J\,mol^{-1}$)	R^2	SD%
283	1.3 ± 0.2	0.812	60.0	3.2 ± 0.3	2.0 ± 0.5	0.980	25.9	2.00 ± 0.05	2.6 ± 0.2	0.986	80.9	50 ± 18	$(4.3 \pm 0.5) \times 10^6$	0.956	23.7
293	1.7 ± 0.2	0.843	53.2	3.6 ± 0.3	2.0 ± 0.5	0.986	20.2	2.23 ± 0.06	2.4 ± 0.2	0.984	10.0	36 ± 10	$(3.6 \pm 0.4) \times 10^6$	0.965	16.4
303	0.6 ± 0.1	0.767	72.9	2.5 ± 0.1	1.7 ± 0.1	0.993	17.3	1.24 ± 0.06	2.3 ± 0.1	0.988	16.2	27 ± 3	$(5.2 \pm 0.2) \times 10^6$	0.972	59.7

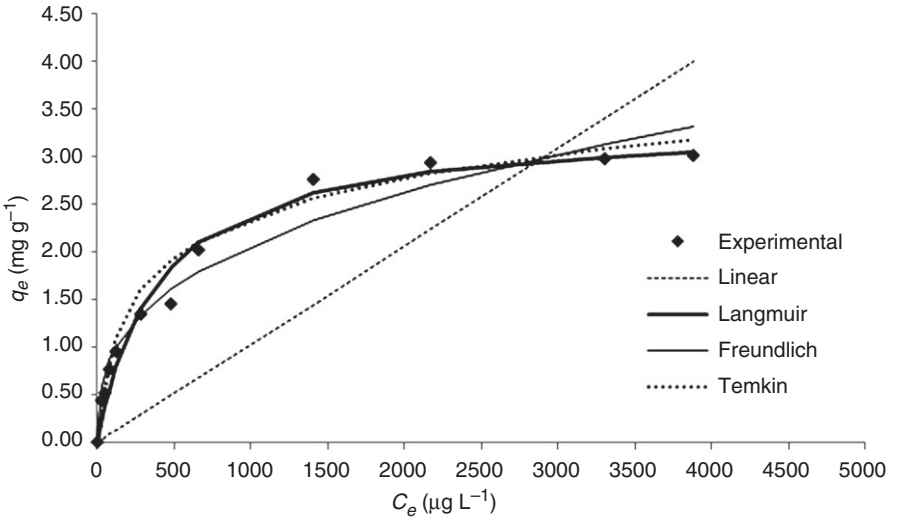

Figure 9. Adsorption isotherms (293K, $d_p < 600\,\mu m$, 120 rpm and contact time of 12 hours).

where R is the gas constant ($8.314\,J\,mol^{-1}\,K^{-1}$), T the absolute temperature (K), A the Temkin isotherm constant ($L\,mg^{-1}$) and b the Temkin constant related to heat adsorption ($J\,mol^{-1}$). This model does not fit the data.

The parameters of all adsorption isotherms are compiled in Table 6. The Langmuir isotherm model had the highest values of R^2, and smaller normalised standard deviations, providing the best approach for equilibrium data (Figure 9). As mentioned, the maximum capacity for monolayer saturation did not change significantly in the range of temperatures studied.

Putra *et al.* [20] reported that equilibrium isotherm data for adsorption of amoxicillin on activated carbon and bentonite were equally well fitted by Langmuir and Freundlich. Once again, this conclusion confirmed the results obtained.

3.9 *Thermodynamic parameters*

In order to confirm the adsorption nature in this study, thermodynamic parameters were determined. Entropy (ΔS°), enthalpy (ΔH°) and Gibbs free energy (ΔG°) were calculated, considering that Langmuir adsorption equilibrium constant is equivalent to q_e/C_e.

Table 7 presents the values of thermodynamic parameters. The enthalpy change is negative, suggesting that the adsorption process is exothermic. The negative value of Gibbs free energy, suggests the spontaneous nature of amoxicillin adsorption onto almond shell ashes. Standard entropy positive determines the increase in disorderliness at solid-liquid interface during the adsorption process.

In other adsorption studies of organic compounds, the thermodynamic parameters were also evaluated. Abramian and El-Rassy [41], Hameed *et al.* [42] and Hameed [37] obtained these parameters for the adsorption of azo-dye orange II onto titania aerogel ($\Delta H^\circ = -16.4\,kJ\,mol^{-1}$, $\Delta S^\circ = -58\,J\,mol^{-1}\,K^{-1}$ and ΔG° (303K) $= 1.2\,kJ\,mol^{-1}$), acidic dye adsorption on activated palm ash ($\Delta H^\circ = 26.6\,kJ\,mol^{-1}$, $\Delta S^\circ = 78\,J\,mol^{-1}\,K^{-1}$ and

Table 7. Thermodynamic parameters for the adsorption of amoxicillin on almond shell ashes.

	Thermodynamic parameters		
T (K)	ΔG (kJ mol^{-1})	ΔH (kJ mol^{-1})	ΔS (J mol^{-1} K^{-1})
283	−89.8		
293	−92.9	−6.7	47.6
303	−96.1		

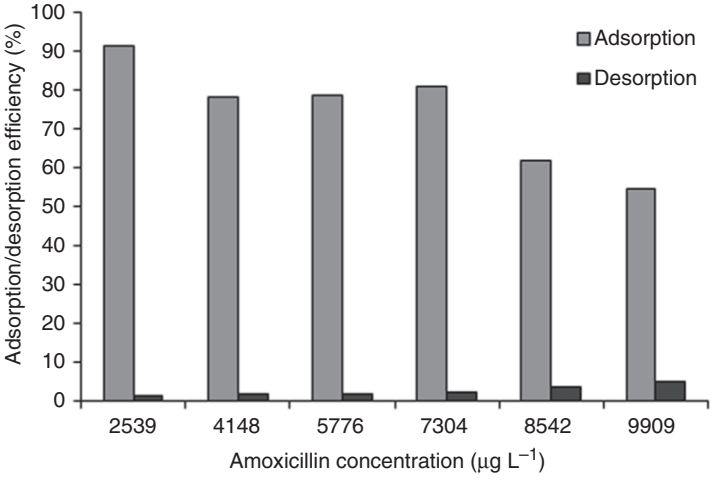

Figure 10. Comparison between adsorption and desorption (50 mg of adsorbent, 303 K, $d_p < 600\,\mu m$, 120 rpm, contact time of 12 hours).

ΔG° (303K) = −0.9 kJ mol^{-1}) and 2,4,6 – trichlorophenol adsorption onto activated clay ($\Delta H^\circ = -9.37$ kJ mol^{-1}, $\Delta S^\circ = -26$ J mol^{-1} K^{-1} and ΔG° (303K) = −1.5 kJ mol^{-1}), respectively.

Comparing these results with those obtained in this study, it was verified that depending on the analyte and the adsorbent material, the adsorption process could be exo- or endothermic, spontaneous or non-spontaneous.

3.10 *Desorption studies*

Desorption assays were carried out in order to estimate the amoxicillin releasing capacity of almond shell ashes. The adsorption and desorption efficiencies were compared in Figure 10. While adsorption efficiency increases with the decrease in initial concentration, the inverse trend seems to occur for desorption. This suggests that when ashes are saturated, amoxicillin is desorbed in a higher extent. It is also important to note that desorption efficiency (maximum desorption of 5%) was quite low, when compared with the adsorption. This is again an indication that there is an irreversible chemical interaction between amoxicillin and almond shell ashes, suggesting chemisorption.

4. Conclusions

The results of this study showed that almond shell ashes may be a good adsorbent for the antibiotic amoxicillin and a good alternative to conventional adsorbents. The adsorption process revealed to be dependent on the amount of adsorbent, initial amoxicillin concentration and adsorbent particle size. Although kinetic data pointed to 400 min as the time necessary to attain 97%, equilibrium data was obtained after 720 min (12 hours). The optimum parameters were 50 mg of adsorbent, 303 K and $d_p < 600\,\mu m$. Experimental results indicated that pseudo-second order kinetics provided the best description of the data. The Langmuir equation provided the best approach for adsorption equilibrium results. Thermodynamic parameters were also evaluated in this study, and revealed that adsorption process was exothermic ($\Delta H^0 < 0$) and spontaneous ($\Delta G^0 < 0$). Finally, desorption revealed a low efficiency (maximum of 5%). The combination of very low desorption efficiencies and the pseudo-second order kinetics as the model that best fits the experimental data suggests that amoxicillin adsorption on almond shell ashes was mainly chemical.

This work intends to be a preliminary study for the subsequent application of this adsorbent in a continuous process (almond shell ashes-packed columns), that should be more closely to the ones employed for treatments at industrial scale.

Acknowledgements

The authors wish to thank the Fundação para a Ciência e a Tecnologia (FCT), Portugal, for financial support (SFRH/BD/38694/2007) and the Centro de Materiais da Universidade do Porto (CEMUP) for XPS and SEM analysis.

References

[1] N. Kemper, Ecol. Indic. **8**, 1 (2008).
[2] M.S. Díaz-Cruz, M.J. López de Alda, and D. Barceló, Trends Anal. Chem. **22**, 340 (2003).
[3] M.D. Hernando, M. Mezcua, A.R. Fernández-Alba, and D. Barceló, Talanta **69**, 334 (2006).
[4] M.I. Bailón-Pérez, A.M. Garcia-Campaña, C. Cruces-Blanco, and M. del Olmo Iruela, J. Chromatogr. A **1185**, 273 (2008).
[5] J.P. Bound and N. Voulvoulis, Chemosphere **56**, 1143 (2004).
[6] M. Ferech, S. Coenen, K. Dvozakova, E. Hendrickx, C. Suetens, and H. Goossens, J. Antimicrob. Chemother. **58**, 408 (2006).
[7] J.M. Cha, S. Yang, and K.H. Carlson, J. Chromatogr. A **1115**, 46 (2006).
[8] A.J. Watkinson, E.J. Murby, D.W. Kolpin, and S.D. Costanzo, Sci. Total Environ. **407**, 2711 (2009).
[9] T.B. Minh, H.W. Leung, I.H. Loi, W.H. Chan, M.K. So, J.Q. Mao, D. Choib, J.C.W. Lam, G. Zheng, M. Martin, J.H.W. Leeb, P.K.S. Lam, and B.J. Richardson, Mar. Pollut. Bull. **58**, 1052 (2009).
[10] X. Pan, C. Deng, D. Zhang, J. Wang, G. Mu, and Y. Chen, Aquat. Toxicol. **89**, 207 (2008).
[11] H. Tekin, O. Bilkay, S.S. Ataberk, T.H. Balta, I.H. Ceribasi, F.D. Sanin, F.B. Dilek, and U. Yetis, J. Hazard. Mater. B **316**, 258 (2006).
[12] B.N. Estevinho, I. Martins, N. Ratola, A. Alves, and L. Santos, J. Hazard. Mater. **143**, 535 (2007).
[13] X.S. Wang, Y. Zhou, Y. Jiang, and C. Sun, J. Hazard. Mater. **157**, 374 (2008).

[14] R. Crisafully, M.A.L. Milhome, R.M. Cavalcante, E.R. Silveira, D. De Keukeleire, and R.F. Nascimento, Biores. Technol. **99**, 4515 (2008).
[15] M. Kazemipour, M. Ansari, S. Tajrobehkar, M. Majdzadeh, and H.R. Kermani, J. Hazard. Mater. **150**, 322 (2008).
[16] E. Pehlivan and T. Altun, J. Hazard. Mater. **155**, 378 (2008).
[17] M. Dutta, N.N. Dutta, and K.G. Bhattacharya, Sep. Purif. Tecnol. **16**, 213 (1999).
[18] H.M. Ötker and I. Akmehmet-Balcığlu, J. Hazard. Mater. **122**, 251 (2005).
[19] K.J. Choi, S.G. Kim, and S.H. Kim, J. Hazard. Mater. **151**, 38 (2008).
[20] E.K. Putra, R. Pranowo, J. Sunarso, N. Indraswati, and S. Ismadji, Water Res. **43**, 2419 (2009).
[21] E. Demirbas, M. Kobya, and A.E.S. Konukman, J. Hazard. Mater. **154**, 787 (2008).
[22] Y. Bulut and Z. Tez, J. Hazard. Mater. **149**, 35 (2007).
[23] F.D. Ardejani, Kh. Badii, N.Y. Limaee, S.Z. Shafaei, and A.R. Mirhabibi, J. Hazard. Mater. **151**, 730 (2008).
[24] B.N. Estevinho, E. Ribeiro, A. Alves, and L. Santos, Chem. Eng. J. **136**, 188 (2008).
[25] B.N. Estevinho, N. Ratola, A. Alves, and L. Santos, J. Hazard. Mater. B **137**, 1175 (2006).
[26] A.F. Goddard, M.J. Jessa, D.A. Barrett, and P.N. Shaw, Gastroenterology **111**, 358 (1996).
[27] J. Rivera-Utrilla, I. Bautista-Toledo, M.A. Ferro-García, and C. Moreno-Castilla, J. Chem. Technol. Biotechnol. **76**, 1209 (2001).
[28] S. Teixeira, C. Delerue-Matos, and L. Santos, J. Sep. Sci. **31**, 2924 (2008).
[29] S.L.R. Ellisson, M. Rosslein, and A. Williams, editors, *EURACHEM/CITAC Guide, Quantifying Uncertainty in Analytical Measurement*, 2nd ed. (EURACHEM/CITAC, Teddington, UK, 2000).
[30] A.D. McNaught and A. Wilkinson, editors, *IUPAC - Compendium of Chemical Terminology*, 2nd ed. (Blackwell Scientific Publications, Oxford, 1997).
[31] D.D. Do, *Adsorption Analysis: Equilibria and Kinetics*, 1st ed. (Imperial College Press, London, 1998), pp. 3–7.
[32] A.P. Terzyk, Colloids and Surfaces A: Physicochem. Eng. Aspects **177**, 23 (2001).
[33] M. Polovina, B. Babić, B. Kaluderović, and A. Dekanski, Carbon **35**, 1047 (1997).
[34] J.-H. Zhou, Z.-J. Sui, J. Zhu, P. Li, D. Chen, Y.-C. Dai, and W.-K. Yuan, Carbon **45**, 785 (2007).
[35] C. Hontoria-Lucas, A.J. López-Penado, J.D. López-González, M.L. Rojas-Cervantes, and R.M. Martín-Aranda, Carbon **33**, 1585 (1995).
[36] G. de la Puente, J.J. Pis, J.A. Menéndez, and P. Grange, J. Anul. Appl. Pyrolysis **43**, 125 (1997).
[37] B.H. Hameed, Colloid. Surface Physicochem. Eng. Aspect **307**, 45 (2007).
[38] M.K. Aroua, S.P.P. Leong, L.Y. Teo, C.Y. Yin, and W.M.A.W. Daud, Bioresour. Technol. **99**, 5786 (2008).
[39] C. Porte, V.C.T. Costodes, H. Fauduet, and A. Delacroix, J. Hazard. Mater. **105**, 121 (2003).
[40] Y.S. Ho and G. McKay, Process Saf. Environ. Prot. **76**, 332 (1998).
[41] L. Abramian and H. El-Rassy, Chem. Eng. J. **150**, 403 (2009).
[42] B.H. Hameed, A.A. Ahmad, and N. Aziz, Chem. Eng. J. **133**, 195 (2007).